OPTIMIZATION OF THE DRYNESS OF GARI PARTICLES IN A FLUIDIZER USING COMPUTATIONAL FLUID DYNAMICS (CFD).

Ejiko, Samuel Omojola[1]; Adefidipe, Ebenezer Rotimi[2]; Adejumo, Samuel Miracle[3]

[1]Department of Mechanical Engineering, The Federal Polytechnic, Ado-Ekiti, Nigeria
[2]Department of Welding and Fabrication, The Federal Polytechnic, Ado-Ekiti, Nigeria
[3]Olusegun Obasanjo Centre for Engineering Innovation, The Federal Polytechnic, Ado-Ekiti, Nigeria

Email: adefidipe_er@fedpolyado.edu.ng

ABSTRACT

This work focuses on the application of Computational Fluid Dynamics (CFD) modeling to optimize the dryness of gari particles in a fluidizer. Gari, a popular staple food in many West African countries, is traditionally made by fermenting and drying cassava tubers. However, the conventional drying methods used in the production process often result in inconsistent dryness levels, which can affect the quality and shelf life of gari. In order to address this issue, a CFD model was developed to simulate the fluid flow and heat transfer within the fluidizer, taking into account the physical properties of the gari particles, air velocity, and temperature. The primary objective was to optimize the drying conditions by achieving uniform and efficient heat transfer throughout the fluidized bed. The CFD model was validated using experimental data obtained from a pilot-scale fluidizer system. These experiments involved varying parameters such as air velocity and temperature to determine their influence on the dryness of the gari particles. The model was successfully able to predict the drying behavior, with good agreement between the simulated and experimental results. The findings of this study demonstrate the potential of using CFD modeling as a tool to optimize the drying process in the gari production industry. By fine-tuning the operating conditions within the fluidizer, producers can achieve more consistent dryness levels, leading to improved product quality and extended shelf life. Additionally, the use of CFD modeling offers a cost-effective and time-efficient approach to optimize the process, reducing the need for extensive trial and error experimentation. Overall, this work sheds light on the benefits of applying computational fluid dynamics modeling in the context of gari particle drying. The insights gained from this study can be extrapolated to other similar food processing industries, where optimizing drying conditions is crucial for product quality and efficiency.

Keywords: CFD Model, Drying, Fluidizer, Gari, Optimization

Introduction

Computational Fluid Dynamics (CFD) is based on the principles of fluid mechanics and uses computers to analyze the behaviors of fluids and physical systems. Computational fluid dynamics (CFD) is a powerful and advanced numerical method to solve governing partial differential equations (PDEs) of mass, momentum, and energy conservation in fluid flow and heat and mass transfer problems (Tomas, and Da-Wen, 2010) . It also could be noted as a useful tool in food engineering problems. CFD was first used in the 1950s and since then, it has been developed increasingly (Tomas, Tiwari. and Da-Wen, 2013) . Computational fluid dynamics (CFD) has been used increasingly to improve process design capabilities in many industrial applications, including industrial drying processes. Drying is a multidisciplinary unit operation which can be expressed as the heart of processing operations in many industries (Narjes, and Seid M., 2018) . Drying of food and beverage products, industrial and municipal wastewater sludge, and other manufacturing and environmental products is done regularly in order to enhance the quality and life span of these products and to facilitate their use, storage, and transportation. The main purpose of drying is reducing the water content of the product in order to reach a safe level to preserve it from deteriorative factors such as microbial, physical and chemical parameters while retaining its sensory and nutritional quality and declining the energy and time consumption and optimization of the process throughput (Bahmani, Jafari, Shahidi, & Dehnad, 2016; Jafari, Ghalegi, & Dehnad, 2017). With recent advancements in mathematical techniques and computer hardware, CFD has been found to be successful in predicting the drying phenomenon in various types of industrial dryers, which utilize all forms of drying operations including spray, freeze, and thermal drying techniques. Understanding the mechanisms underlying the drying processes has a critical role in dehydration of food and agricultural products. Advanced computer modeling and simulation techniques can help in developing new dryers, modification of current systems, energy saving and process optimization. Also the most important parameter during the drying food products is food quality (moisture content, crack formation, case hardening, etc.) which can be enhanced through using appropriate modeling. Computational Fluid Dynamics (CFD) is a well-known modeling technique which has received more attention in the food industry in the recent years. Hydrodynamics of fluid flow, heat and mass transfer during drying can be predicted using CFD (Narjes, and Seid, 2018).

The CFD solutions are being used to optimize and develop equipment and processing strategies in the drying industry, replacing expensive and time-consuming experimentations. The CFD modeling tools are used to predict the detailed three-dimensional behavior of liquid, gas and particles flow. Drying process is one of the old methods to

preserve and prevent damage of food that produces dry product with good quality (Doymaz, 2004). Drying is a complex process involving mass and heat transfer and between products and the environment that reduces the moisture content in the product (Aviara, Onuoha, Falola, and Igbeka, 2014). Fluidized bed dryer is one of the dryers that is widely used in chemical industry, food, and pharmaceuticals for drying powdered or granular material (Palzer, 2007). Computational Fluid Dynamics (CFD) is a computational technology that enables researchers to study the dynamics of things that flow. By using CFD, it is possible to build a computational model that represents a system under study. It not only predicts fluid flow behavior, but also the transfer of heat, mass, phase change, chemical reaction, mechanical movement, and stress or deformation of related solids (Nazghelichi, 2013).

A fluidizer is an apparatus that is used to extract saturated solid or thickened material from a storage device such as a wet cassava flakes (gari) during processing. Gari is a granulated white and yellow product from cassava depending on production method. Gari is fermented gelatinized dry coarse flour, very popular in West Africa and a staple food in Nigeria, Ghana, and Togo. (Ejiko, Oigbochie and Emmanuel, 2018) Gari frying is a complex procedure which in traditional processing depends for its success almost entirely on the skill of the operator. A tradition fire place consists of three stones supporting the frying pan (Ismail, Ojolo, Olatunji, and Ogunleye, 2012). This causes a great deal of discomfort to the operators due to exposure to heat and smoke from the fire and steam from the wet cassava mash. At the same time the system is very inefficient in its use of fuel, energy consumption per unit of dried gari is considered to be too high. Even enclosing the fire on three sides will improve fuel consumption and reduce smoke blowing into the faces of the operator. The efficiency and effectiveness of frying and fire wood consumption are the most important issues in tradition production that need to be addressed most urgently (Ismail et al., 2012).

Materials and Methods

Materials

The research made use of a fabricated gari frying system and SOLIDWORKS App for design and modelling

Methodology for CAD design

i. Experimented works were carried out on a fabricated fluidizing chamber of a gari processing machine
ii. Application of solidworks to analyze and stimulate the design of the fabricated fluidizer

CFD Modelling Methods

Following conditions are considered for running CFD Model

1. Definition of the system unit
2. Definition of analysis type
3. Definition of fluid type
4. Definition Wall condition
5. Definition initial condition

Solid works Simulation Procedure

After completing the CAD drawing and assembly, the flow simulation in Solidworks was initiated by loading the relevant add-in. This action led to the display of the flow simulation form, wherein the wizard was then clicked on within the flow simulation page. By doing so, an interface was provided, allowing for the configuration of various parameters required for the simulation.

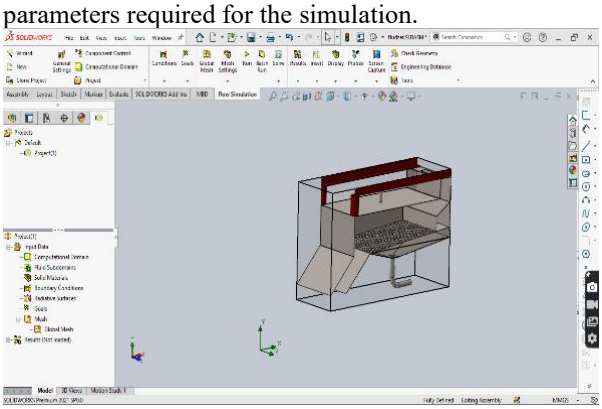

Figure 1: CFD model interface

In every CFD analysis, it is necessary to go through several steps to build the computational model, carry out the computation, and analyze the results as follows:

1. The Wizard option was clicked on.
2. The work name was established.
3. The system unit definition was selected with SI units: meters (m) for length, kilograms (kg) for weight, and seconds (s) for time.
4. Heat conduction in solids was chosen as the simulation type since the fluidizer comprised stainless steel. The metal's potential for heat absorption when exposed to hot air necessitates consideration of its material, as well as gravity.
5. The internal analysis type was designated with physical features like heat conduction in solid body and gravity.
6. The default fluid was selected, with air as the medium present in the fluidizer.
7. The type of flow was selected from options, including laminar turbulent, humidity, and high mash number of flow.
8. Word conditions were established using default values, with adiabatic work as the default thermal condition - 101325p for

initial pressure and 293.2k for initial temperature.

9. Boundary conditions were defined automatically for the system domain, with inlet volume flow at 0.00333m^3/s and m^3/s environmental conditions.
10. The fluidizer has an entry hopper for gari, an exit, and an exhaust pipe that serves as a pressure relief port. The user established the entry and exit points for the gari, which operate as a second boundary condition.
11. The CFD system started running.

Experimental methodology

The gari undergoes several processing stages to get to the final product. The process involves breaking, sieving, cooking, and drying.

Stage one:

The first stage is breaking and sieving.

In the initial stage, the dewatered gari undergoes breaking and sieving processes. This involves utilizing a machine equipped with a hopper, spike for breaking lumps, sweeper for removing impurities, and a mesh for sieving the gari. The machine is powered by an electric motor.

Stage two:

Cyclone: Temporary storage.

Moving on to Stage Two, we have the cyclone, which serves as a temporary storage facility. In this stage, the filtered gari from Stage One is safely stored in the cyclone, allowing it to be held until it's required for the subsequent step. When the gari is needed, it can be released from the cyclone at a carefully controlled rate.

Stage three:

Cooking chamber

At this stage, Water Jacket Cooking Chamber is utilize to provide controlled heating and cooking for the gari as shown in figure 2. Within this chamber, the filtered gari is carefully introduced into the inner chamber. The hot water jacket, surrounding the inner chamber, indirectly transfers heat to evenly and thoroughly cook the gari. A conveyor system is incorporated to aid the cooking process via smoothly conveying the gari from the entry to the exit of the cooking chamber. This system is equipped with an electric heater boasting a capacity of 2000 watts, alongside an electric motor to power its operations.

Final stage:

Drying Equipment (Fluidization).

Following the cooking process, the gari undergoes drying in a fluidization system. This system involves exposing the cooked gari to hot, pressurized air, which removes moisture and propels the gari through the equipment. This process results in gari with a low moisture content, which is essential for its long-term storage and commercial viability.

Figure 2: cooking in cooking chamber with heater

Finding analysis

The type of fluidizer used is called flash reactor (transport reactor). Sand bed materials will be considered

Bed pressure drop Δp_w

Parameters needed in fluidization

dp = particle diameter (m)

D_0 = bottom diameter of the tapered bed (m)

D_1 = top diameter of the tapered bed (m)

H_s = stagnant height of the particle bed (m)

Δ p_{max} = minimum pressure drop through the particle bed (Pa)

Greek symbols

ρ_f = fluid density (kgm^3)

ρ_s= solid density (kgm^3)

To find P_{max}, an empirical formula in equation 1 as given by Sau, Mohanty and Biswal (2007) was applied

$$P_{max} = 7.457 \left(\frac{D_1}{D_0}\right)^{0.038} \left(\frac{d_P}{D_0}\right)^{0.222} \left(\frac{H_s}{D_0}\right)^{0.642} \left(\frac{P_s}{P_f}\right)^{0.723} \quad (1)$$

$$P_{max} = 7.457 \left(\frac{1.2}{0.2}\right)^{0.038} \left(\frac{0.000717}{0.2}\right)^{0.222} \left(\frac{0.1}{0.2}\right)^{0.642} (2573)^{0.723}$$

$= 7.457\ (6)^{0.038}\ (0.0035)^{0.222}\ (0.5)^{0.642}\ (2573)^{0.723}$

$= 7.457\ (1.07)\ (0.25)\ (0.64)\ (292)$

$= P_{max} = 417.5pa$

To determine the mass of Gari that can be fluidized by the P_{max} from the fluidizing bed

$A = L \times B$ (2)

$= 0.6 \times 0.02 \quad = 0.012m^2$

A = Area covered by the gari coming from the cooking chamber

P = F/A

417 = F/0.012

F = 417 × 0.012

F = 5.004N

F = 0.5kg

Cost Implication

After the three phases have been completed, the machine was subjected to testing and running in order to see the outcome and its effective result.

The overall cost of the work is #1,700,000 concerning all the tools, printing, and parts needed

for the completion of the work as shown in Table 1. Some items were ordered from the engineering store and the duration for the delivery were not in any case affect the progress of the work.

Table 1: Estimates of automated fluidizing bed

S/N	Material	Qty	Rate (#)	Amount (#)
1	Cooking Chamber Modification	1	400,000	400,000
2	Fluidizer modification	1	700,000	700,000
2	Control	-	250,000	250,000
3	CFD simulation	-	350,000	350,000
			Total	1,700,000

Results and Discussion

CFD simulation result

The following result was obtained from the CFD simulation using SOLIDWORKS flow simulation. The selected units, analysis type, and a referred axis for the CFD. Temperature and pressure flow interface captured in figures 3 to 5

The Table 2 and probably 3 and 4 shows the selected units, analysis type, and a referred axis for the CFD:

Table 2: General Information of the CFD simulation

Model	Fluidizer
Work name	Fluidizer CFD
Units system	SI (m)(kg)(s)
Analysis type	Internal
Exclude cavities without flow conditions	Off
Coordinate system	Global Coordinate System
Reference axis	X

Physical Features of the simulation

Heat conduction in solids: On
Heat conduction in solids only: Off
Radiation: Off
Radiation in gases: Off
Time dependent: On
Gravitational effects: On
Rotation: Off
Flow type: Laminar and turbulent
High Mach number flow: Off
Humidity: Off
Free surface: Off
Default roughness: 0 micrometer

Table 3; Gravitational Settings for the simulation

X component	0 m/s^2
Y component	-9.81 m/s^2
Z component	0 m/s^2

Outer wall condition: Adiabatic wall

Table 4: Initial Conditions of outer wall

Thermodynamic parameters	Static Pressure: 101325.00 Pa Temperature: 293.20 K
Velocity parameters	Velocity vector Velocity in X direction: 0 m/s Velocity in Y m direction: 0 /s Velocity in Z direction: 0 m/s
Solid parameters	Default material: Steel Stainless 302 Initial solid temperature: 293.20 K
Turbulence parameters	Turbulence intensity and length Intensity: 2.00 % Length: 0.006 m

Material Settings for the simulation

Fluids: Air

Solids: Steel Stainless 302

Table 5 and 6 present the details of inlet volume flow and environmental pressure respectively. Table 7 shows the boundary conditions used for the simulation.

Table 5: Inlet Volume Flow

Type	Inlet Volume Flow
Faces	fluidizer inlet lid-1/Revolve1//Face
Coordinate system	Face Coordinate System
Reference axis	X
Flow parameters	Flow vectors direction: Normal to face Volume flow rate: 0.0033 m^3/s Fully developed flow: Yes
Thermodynamic parameters	Approximate pressure: 101325.00 Pa Temperature type: Temperature of initial components Temperature: 773.20 K

Table 6: Environment Pressure

Type	Environment Pressure
Faces	fluidizer outlet lid-1/Boss-Extrude1//Face fluidizer outlet lid 3-1/Boss-Extrude1//Face fluidizer outlet lid 2-1/Boss-Extrude1//Face
Coordinate system	Global Coordinate System
Reference axis	Y
Thermodynamic parameters	Environment pressure: 101325.00 Pa Temperature type: Temperature of initial components Temperature: 293.20 K
Turbulence parameters	Turbulence intensity and length Intensity: 2.00 % Length: 0.006 m
Boundary layer parameters	Boundary layer type: Turbulent

Table 7: Results From the Simulation

Name	Minimum	Maximum
Density (Fluid) [kg/m^3]	0.46	1.20
Density (Solid) [kg/m^3]	7900.00	7900.00
Pressure [Pa]	101303.95	101316.23
Temperature [K]	293.14	973.20
Temperature (Fluid) [K]	293.14	973.20
Temperature (Solid) [K]	293.20	298.77
Velocity [m/s]	0	4.401
Velocity (X) [m/s]	-4.383	1.302
Velocity (Y) [m/s]	-0.128	3.167
Velocity (Z) [m/s]	-1.341	1.257
Domain Index (Solid) [ ]	3	4
Mach Number [ ]	0	8.02e-03
Velocity RRF [m/s]	0	4.401
Velocity RRF (X) [m/s]	-4.383	1.302
Velocity RRF (Y) [m/s]	-0.128	3.167

Velocity RRF (Z) [m/s]	-1.341	1.257
Vorticity [1/s]	2.19e-06	297.29
Relative Pressure [Pa]	-21.05	-8.77
Shear Stress [Pa]	0	0.03
Solid Thermal Conductivity (X) [W/(m*K)]	16.3000	16.3000
Solid Thermal Conductivity (Y) [W/(m*K)]	16.3000	16.3000
Solid Thermal Conductivity (Z) [W/(m*K)]	16.3000	16.3000
Specific Heat (Solid) [J/(kg*K)]		500.0
Bottleneck Number [ ]	0	1.0000000
Heat Flux [W/m^2]	8.838e-11	29390.537
Heat Flux (X) [W/m^2]	-29169.348	3310.002
Heat Flux (Y) [W/m^2]	-3964.687	3535.266
Heat Flux (Z) [W/m^2]	-3805.857	3847.873
Heat Transfer Coefficient [W/m^2/K]	0	1171934.629
Overheat above Melting Temperature [K]	-1379.951	-1374.376
Shortcut Number [ ]	0	1.0000000
Surface Heat Flux [W/m^2]	-15444.996	8.372
Surface Heat Flux (Conductive) [W/m^2]	0	0
Surface Heat Flux (Convective) [W/m^2]	-15444.996	8.372
Total Enthalpy Flux [W/m^2]	-12099.954	1602968.443
Acoustic Power [W/m^3]	0	1.051e-17
Acoustic Power Level [dB]	0	0

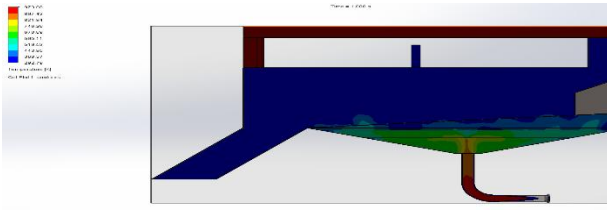

Fig. 3: Temperature result from the simulation

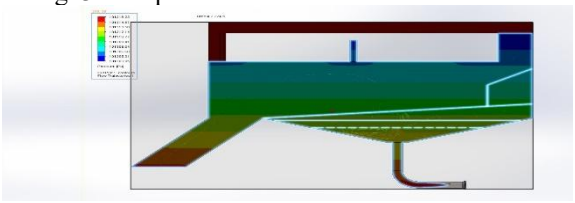

Fig. 4: CFD Pressure gradient across fluidizer surface area

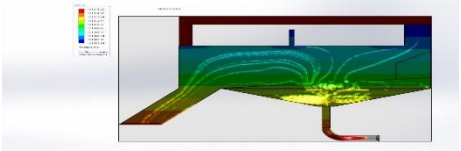

Fig. 5: CFD Pressure Result Chart Showing flow direction

Table 8: Temperature result gotten from the simulation.

S/N	Inlet temperature (°c)	Fluidizer inner temperature (°c)
1	500	85
2	600	94
3	700	116
4	800	120
5	900	124

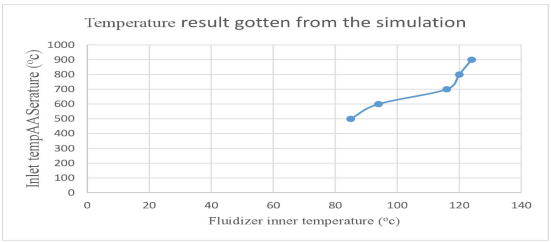

Fig. 6: Temperature result gotten from the simulation.

CFD Result Discussion

The simulation was based on one parameter of the fluidizer, the fluidizing temperature. Other factors such as pressure and air-flow rate were also considered. Environmental pressure was considered and 300 m^3/s flow rate of air was considered in the simulation.

Table 2 presents the General Information of the CFD simulation, providing a summary of the simulation settings. In Table 3, the Gravitational Settings for the simulation are displayed. Table 4 highlights the Initial Conditions of the outer wall, while Table 5 showcases the Inlet Volume Flow. Environment Pressure is depicted in Table 6, and Table 7 presents the results obtained from the simulation, Table 8 presents the results obtained from a simulation showing the relationship between different Inlet Temperatures and the corresponding Fluidizer Inner Temperatures. The Inlet Temperature, measured in degrees Celsius (°C), represents the temperature at the entrance of the system, while the Fluidizer Inner Temperature, also measured in degrees Celsius (°C), is the temperature within the fluidizer.

The data indicates that as the Inlet Temperature increases, there is a corresponding increase in the Fluidizer Inner Temperature. For instance, at an Inlet Temperature of 500°C, the Fluidizer Inner Temperature was 85°C, while at an Inlet Temperature of 900°C, the Fluidizer Inner Temperature increased to 124°C.

This information provides insight into the thermal behavior of the system and how changes in the Inlet Temperature impact the internal temperature of the fluidizer.

Moving on to the figures, Fig. 3 illustrates the temperature gradient within the chamber, showcasing how the temperature decreases towards the upper part of the fluidizer. Fig. 4 exhibits the distribution plate of the fluidizing chamber, where pressurized air is evenly distributed. Fig. 5 illustrates the pressure gradient within the chamber, showcasing how the pressure decreases towards the upper part of the fluidizer. This phenomenon facilitates the fluidization process of the gari. Furthermore, Fig. 5 displays the direction of the airflow, suggesting that the fluidizing chamber is capable of both drying and conveying the gari from the entry point to the discharge point.

Table 8 presents the temperature results obtained from a simulation. The "S/N" column represents the serial number of each data entry, while the "Inlet temperature (°C)" column shows the introduced temperature into the fluidizer. The "Fluidizer inner temperature (°C)" column displays the corresponding temperature achieved inside the fluidizer during the simulation.
For example, the first row indicates that when the heat entered the fluidizer at 500°C, the inner temperature of the fluidizer reached 85°C. Similarly, the subsequent rows display the inlet temperatures and the resulting inner temperatures of the fluidizer for each simulation run.

4.3 Result from Experiment

Table 9 shows the temperature and moisture content of the fluidized bed and cooked gari of 1kg

S/N	Inlet temperature (°c)	Fluidizing Temperature (°c)	Final Mass (kg)	Final Moisture content (%)
1	498	80	0.83	83
2	595	90	0.74	74
3	698	100	0.66	66
4	785	110	0.57	57
5	894	120	0.49	49

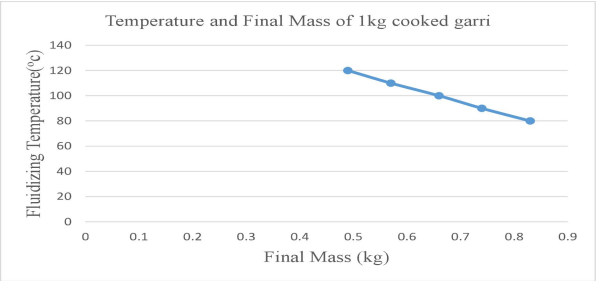

Fig. 6: Temperature and Final Mass of 1kg cooked gari

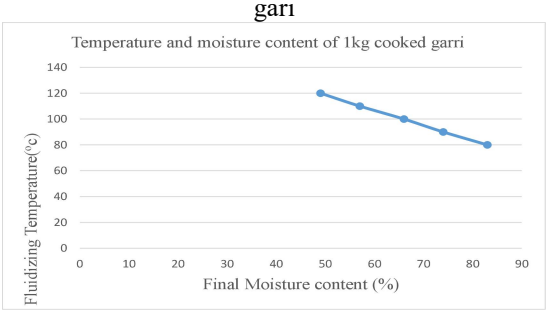

Fig. 7: Temperature and moi

Table 10 shows the temperature and moisture content of fluidized bed and cooked gari 2kg

S/N	Inlet temperature (°c)	Fluidizing Temperature(°c)	Final Mass (kg)	Final Moisture content (%)
1	498	80	1.75	87.5
2	595	90	1.66	83.0
3	698	100	1.58	79
4	785	110	1.49	74.5
5	894	120	1.18	59

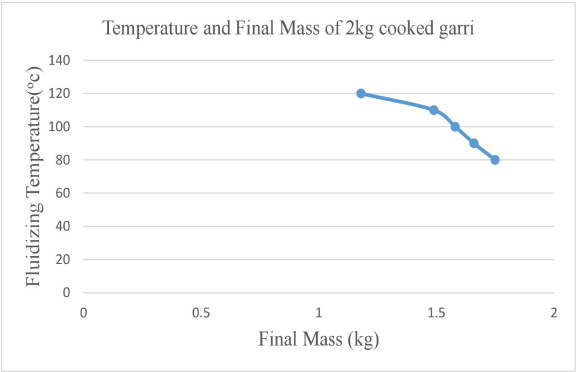

Fig. 8: Temperature and Final Mass of 2kg cooked gari

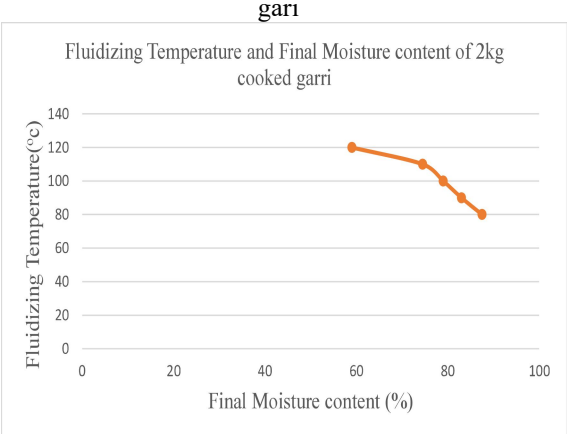

Fig. 9: Fluidizing temperature and Final Moisture content of 2kg cooked gari

Table 11 shows the temperature and moisture content of fluidized bed and cooked gari 3kg

S/N	Inlet temperature (oc)	Fluidizing Temperature (°c)	Final Mass (kg)	Final Moisture content (%)
1	498	80	2.79	93
2	595	90	2.31	77
3	698	100	2.04	68
4	785	110	1.98	66
5	894	120	1.56	52

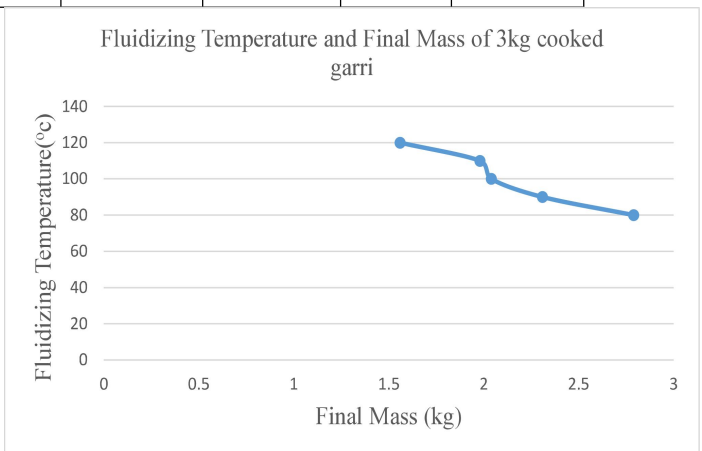

Fig. 10: Fluidizing temperature and Final Mass of 3kg cooked gari

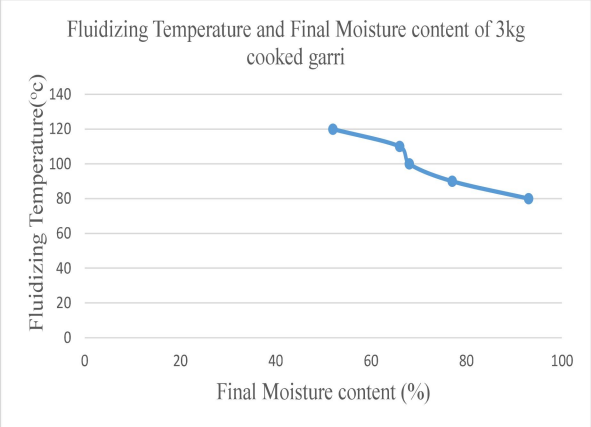

Fig. 11: Fluidizing temperature and Final Moisture content of 3kg cooked gari

Table 12: shows the temperature and moisture content of fluidized bed and cooked gari 4kg

S/N	Inlet temperature (oc)	Fluidizing Temperature (°c)	Final Mass (kg)	Final Moisture content (%)
1	498	80	3.81	95.25
2	595	90	3.53	88.25
3	698	100	2.91	72.75
4	785	110	2.46	61.50
5	894	120	2.13	53.25

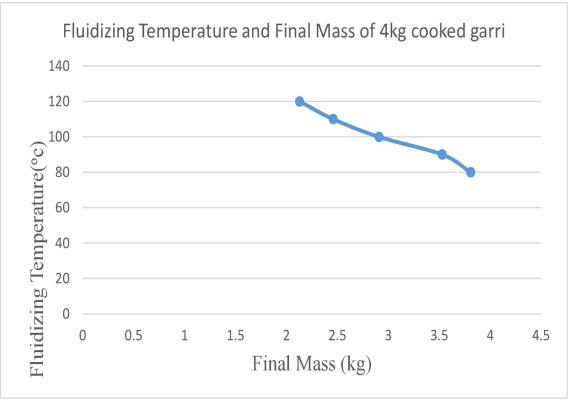

Fig. 12: Fluidizing temperature and Final Mass of 4kg cooked gari

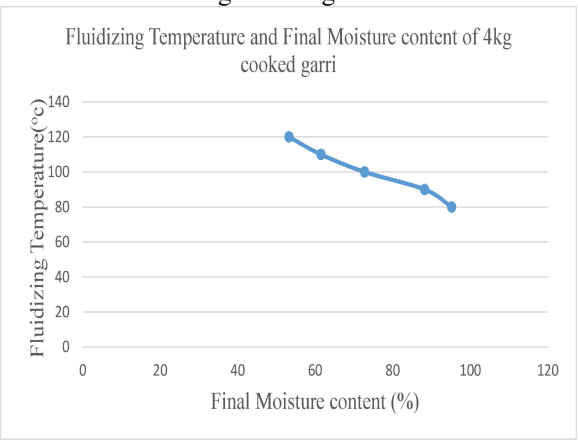

Fig. 13: Fluidizing temperature and Final Moisture content of 4kg cooked gari

Fig 14: Data logger display screen

The Experimental Results Discussion

The result gotten from the local frying system reveals that 90°C was the frying temperature. Having a higher temperature will bring more effectiveness to the drying operation.

The fluidizing experiment aimed to achieve temperatures of 80°C, 90°C, 100°C, 110°C, and 120°C inside the fluidizer. In order to achieve this, a data logger was programmed to automatically save and update whenever the targeted temperature was reached inside the fluidizer, while also recording the corresponding inlet temperature required to achieve the desired temperature. The obtained results showed that the inlet temperatures reached were 498°C, 595°C, 698°C, 785°C, and 894°C, resulting in temperatures of 80°C, 90°C, 100°C, 110°C, and 120°C respectively inside the fluidizer.

The experimental findings revealed an inverse relationship between the fluidizing temperature and the final mass/moisture content during the drying process of gari. These results suggest that higher fluidizing temperatures lead to increased moisture removal, resulting in reduced final mass and moisture content. This insight has potential applications in optimizing drying processes and material treatments, as higher fluidizing temperatures facilitate enhanced moisture evaporation due to increased energy input.

Temperature plays a crucial role in expediting the moisture evaporation process from a material during drying. This relationship is commonly depicted through a drying curve, which illustrates the decrease in moisture content of a material under specific drying conditions. The initial stage of drying, known as the constant rate period, is characterized by a rapid decrease in moisture content as the material approaches or reaches its saturation point. The elevated temperature aids in breaking the bonds between water molecules, enabling them to escape more readily.

Furthermore, the mass of the gari decreases as temperature rises, reflecting the removal of moisture content. Ultimately, heightened temperatures contribute to more effective drying of the gari, resulting in reduced mass and moisture content at the conclusion of the process.

Understanding the impact of temperature on mass and moisture content is crucial for optimizing industrial processes such as drying, where precise control of these parameters is essential to achieve desired product characteristics. Exploring the specifics of this relationship could provide insights into the kinetics of moisture removal and the thermodynamics of the drying process, potentially leading to improved energy efficiency and throughput in drying operations, thereby influencing cost and resource utilization.

Conclusion

In this study, we investigated the application of Computational Fluid Dynamics (CFD) modeling to optimize the dryness of Gari particles in a fluidizer. Specifically, we focused on analyzing the effects of input temperature and temperature inside the fluidizer on the drying process, the application of Computational Fluid Dynamics (CFD) model in optimizing the dryness of gari particles in a fluidizer has shown promising results. Through the simulation and experimental analysis, the effects of input temperature of 700 ºc from blower, due to effect of distribution plates and the walls of the fluidizer which cause the temperature above the fluidize bed to drop to about 116 ºc. The result from the CFD which was transferred to the physical testing of the fluidizer was able to increase the temperature of the cooked gari which was introduced at the temperature of 64 ºc into the fluidizing chamber to about 98 ºc which was about 25% moisture content removal. The result given from the CFD was able to optimize the effects of drying in the fluidizing chamber.

In summary, the application of Computational Fluid Dynamics (CFD) model to optimize the dryness of gari particles in a fluidizer has shown great potential. The findings from both simulation and experiment emphasize the importance of controlling input temperatures and managing temperature distribution within the fluidizer for achieving desired levels of dryness. This research opens up new avenues for further exploration and improvement in gari drying processes, benefiting the food processing industry as a whole.

Recommendations

Based on the analysis conducted using CFD, it is recommended to further explore the application of CFD in optimizing the dryness of gari particles in a fluidizer. Additionally, the following recommendations are proposed:

1. Conduct further experimental studies: While CFD provides valuable insights into the fluid dynamics and drying behavior of gari particles in a fluidizer, it is essential to validate these findings through experimental studies. This will help to ensure the accuracy and reliability of the results obtained from
2. Optimize fluidizer design parameters: Through CFD simulations, various fluidizer design parameters such as fluid velocity, particle size distribution, and inlet temperature can be studied to identify the optimal conditions for achieving maximum dryness. The findings from these simulations can then be used to improve the design of the fluidizer and enhance the overall efficiency of the drying process.
3. Implement feedback control systems: By integrating CFD with real-time data acquisition systems, it is possible to develop feedback control systems that can dynamically adjust the operating parameters of the fluidizer. This can lead to better control over the drying process and facilitate the achievement of desired gari particle dryness levels.
4. Investigate alternative drying techniques: While CFD provides valuable insights into the fluid dynamics within a fluidizer, it may be beneficial to explore alternative drying techniques. Comparing the performance and efficiency of different drying methods, such as spray drying or freeze drying, can provide a more comprehensive understanding of the optimal approach for achieving the desired dryness of gari particles.
5. Consider the effect of operating conditions: CFD simulations can be used to analyze the impact of various operating conditions, such as heat transfer mechanisms, residence time, and airflow rates, on the drying process. By systematically varying these parameters, it is possible to identify the most influential factors and their optimal range for achieving the desired gari particle dryness.
6. Develop predictive models: CFD can be used to develop predictive models that can estimate the drying behavior and dryness of gari particles based on input parameters. These models can serve as valuable tools for process optimization, allowing for quick and reliable predictions of dryness under different operating conditions without the need for extensive experimentation.

CONTRIBUTION TO KNOWLEDGE

This work is to optimize to functionality of a fluidizer. Instead of running multiple experiments to know the amount of airflow rate that can generate the appreciable pressure to fluidize, the CFD model can easily give out the result without

stress. This model removes the stress of running multiple physical experiments in order to achieve a particular objective in fluid analysis

REFERENCES

Bahmani, A., Jafari, S. M., Shahidi, S. A. & Dehnad, D. (2016). Mass Transfer Kinetics of Eggplant during Osmotic Dehydration by Neural Networks. *Journal of Food Processing and Preservation, 40*(5). doi:10.1111/jfpp.12435

Doymaz, I. (2004). Convective air drying characteristic of thin layer carrots. *Journal of Food Engineering, 61*(3), 359-364. doi:10.1016/S0260-8774(03)00142-0

Ejiko, S. O., Oigbochie D. and Emmanuel, A. A. (2018). Design of a Semi Mechanize Gari Fryer. *IOSR Journal (IOST-JMCE), 15*(2), 49-59.

Ismail, S. O., Ojolo, S. J., Olatunji, O. O. and Ogunleye, I. O. (2012). DESIGN AND DEVELOPMENT OF A CONTINUOUS FLUIDIZED-BED GARI DRYER. *International Journal of Engineering Innovations, 4*(3). Retrieved from www.panafricanjournal.org

Jafari, S. M., Ghalegi, G., & Dehnad, D. (2017). Influence of spray drying on water solubility index, apparent density, and anthocyanin content of pomegranate juice powder. *Powder Technology*, 311. doi:10.1016/j.powtec.2017.01.070

Narjes, and Seid M. (2018). Simulation of food drying processes by Computational Fluid Dynamics (CFD); recent advances and approaches. *Trends in Food Science & Technology*, 206-223.

Nazghelichi. (2013). Hydrodynamics behavior of a laboratorial fluidized bed dryer containing carrot cubes as well as heat transfer in the dryer. *J. Chem. Chem. Eng*.

Ndubisi A. Aviara, Lovelyn N. Onuoha, Oluwakemi E. Falola and Joseph C. Igbeka. (2014). Energy and exergy analyses of native cassava starch drying in a tray dryer. *Energy, 73*(C), 809-817. doi:10.1016/j.energy.2014.06.087

Palzer, S. (2007). Drying of wet agglomerates in a continuous fluid bed: Influence of residence time, air temperature and air-flow rate on the drying kinetics and the amount of oversize particles. *Chemical Engineering Science, 62*(1-2), 463-470. doi:10.1016/j.ces.2006.09.032

Sau, D. C., Mohanty, S., Biswal, K. C. (2007). Minimum Fluidization Velocity and Maximum Bed Pressure Drops for Gas-Solid Tapered Fluidized Beds. *Chemical Engineering Journal, 132*(1-3).

Tomas, and Da-Wen. (2010). CFD: An Innovative and Effective Design Tool for the Food Industry. *Food Engineering at Interfaces*.

Tomas, Tiwari. and Da-Wen. (2013). Computational Fluid Dynamics in the Design and Analysis of Thermal Processes: A Review of Recent Advances. *Critical Reviews In Food Science and Nutrition 53(3)*, 251-75.